RAPID COMMUNICATIONS

PHYSICAL REVIEW B VOLUME 32, NUMBER 7 1 OCTOBER 1985

Density and size of neon bubbles in molybdenum, tantalum, and tantalum oxide

A. Luukkainen, J. Keinonen, and M. Erola
Accelerator Laboratory, University of Helsinki,
Hämeentie 100, SF-00550 Helsinki, Finland
(Received 3 July 1985)

The density and size of neon bubbles have been studied for the fluences of 6.2×10^{19} to 9.4×10^{21} 60-keV ($^{22}Ne^+$ ions)/m^2 in the bcc metals Mo and Ta and in the amorphous Ta_2O_5 by means of the Doppler-shift attenuation method through the reaction $^{22}Ne(p,\gamma)^{23}Na$. The concentration dependence of the bubble size was determined. Atomic Ne densities within the bubbles derived from the bubble sizes indicate overpressurized Ne bubbles in Mo and Ta in contrast to thermal equilibrium bubbles in Ta_2O_5.

In the gas-ion implantation of metals, the fluence range of 10^{18} to 10^{21} ions/m^2 is characterized by complete trapping and clustering of the implanted gas in the damage within the ion range.[1] Due to the very low solubility of inert gases in metals,[2] the clustering of occupied trapping sites leads already at low concentrations to the formation of gas-filled bubbles. In spite of the fact that He bubbles have been studied by several authors, the information about the growth of the bubbles below the blistering limit is scarce and, about the overpressurized bubbles, controversial.[1] The information about bubbles of heavier inert gases is limited to a few studies on blistering and flaking,[1] and to our knowledge only one study is reported on the pressure,[3] but no studies on the growth and density of gas bubbles below the blistering limit (the fluence range 10^{18} to 10^{21} ions/m^2).

In this study we report for the first time on extensive data concerning the concentration dependence of the bubble density and the size and atomic density of bubbles of a heavier inert gas in metals. A new method [the Doppler-shift attenuation (DSA) method], in conjunction with the experimentally known concentration distributions, has been used to study neon bubbles in the bcc metals Mo (the DSA data is from a previous work[4]) and Ta and, for comparison, in the amorphous material Ta_2O_5 as a function of the implanted dose, ranging from an atomic concentration of about one percent to a saturation value. We emphasize the concentration rather than dose or fluence dependence in the description of the properties of Ne bubbles for the following reasons: (i) Because the implantation of inert gases heavier than He produces high sputtering of metals[5] the amount of retained gas (dose) is lower than the fluence and saturates at rather low fluences. (ii) The Ne concentration at a given dose is dependent on the implantation energy also affecting the sputtering yield. The information on neon bubbles (bubble density, size, and atomic density of neon bubbles) is extracted by Monte Carlo calculations reproducing the DSA data and concentration distributions.

The DSA method has been conventionally used in our laboratory to deduce the mean lifetime τ of recoiling, γ-emitting nuclei formed by the (p,γ) reaction between the implanted target atoms and a beam of high-velocity protons.[6] In the case of a known lifetime, the velocity of the recoiling nuclei at the moment of the γ-ray emission depends on the stopping power of the slowing-down material. The change in the velocity due to the changes of the stopping conditions (bubble density, size, and atomic density) can be obtained from the F factor, which is the ratio between the recoil atom's velocity component along the beam direction and the original velocity. How different amounts of implanted target material ^{22}Ne affect the $F(\tau)$ value is shown in Table I and illustrated in Fig. 1. The ^{22}Ne samples were prepared by implanting at room temperature 60-keV $^{22}Ne^+$ ions into polycrystalline Mo and Ta and 5000-Å-thick, amorphous Ta_2O_5 (electrolytically oxidized). The $F(\tau)$ values were measured for the 2.64-MeV state in ^{23}Na. The lifetime 119 ± 5 fs is in the region where the $F(\tau)$ value obtained through the $^{22}Ne(p,\gamma)^{23}Na$ reaction at $E_p=1005$ keV is most sensitive to the changes in the slowing-down conditions. The experimental methods in obtaining the dose and maximum concentration (the collection curve) and the $F(\tau)$ value have been explained previously.[4] Neon bubbles used in the Monte Carlo simulation of the $F(\tau)$ values are briefly discussed in the following.

Because the $F(\tau)$ value is affected by all retained Ne atoms, the bubble density and size to be determined include both Ne trapped in microscopic bubbles and Ne clusters in submicroscopic cavities. According to the experimental data[7-9] on He in Ni, Al, and Cu, the bubble density C_b [(Ne bubbles)/Å^3] was taken to be constant below the concentration limit of the bubble coalescence. It was a fitting parameter in reproducing the $F(\tau)$ values. In the calculations, the bubble radius was varied with the experimentally known concentration distribution along the path of recoiling ^{23}Na atoms. Thus, the bubble radius $\bar{r}_b$ is the mean radius at a constant concentration. The values of $\bar{r}_b$ were obtained by reproducing the concentration distributions and doses. The effect of Ne atoms not contained in the microscopic or submicroscopic bubbles was estimated by assuming their fraction to be half of the Ne dose. (According to the He data,[1] this is, in the present case where submicroscopic bubbles are also included, a very conservative upper limit in approaching this open question.) It was observed that C_b would be reduced to half of the original value, but $\bar{r}_b$ increased by only 20%.

The pressure-radius relationship of bubbles at the mechanical stability limit is given[10] by

$$p=\frac{2\gamma}{r_b}+\frac{\mu b}{r_b}\ , \tag{1}$$

where γ is the specific surface free energy, μ the shear modulus of the metal matrix, and b the magnitude of the Burgers vector of dislocation loops. As the values $\gamma\approx1$ J m^{-2}, $\mu\approx10^{11}$ J m^{-3}, and $b\approx2$ Å are typical for all metals,[11] the $\bar{r}_b-n_{Ne}$ relationship was approximated by the

 ©1985 The American Physical Society

TABLE I. Summary of the samples, $F(\tau)$ values (%), and results obtained for the mean radii $\bar{r}_b$ and $\langle \bar{r}_b \rangle$ (Å) and atomic densities n_{Ne} (Å^{-3}) of Ne bubbles. The implanted fluence ϕ is given in units of 10^{20} ions/m^2, dose D in 10^{20} atoms/m^2 and maximum concentration C_{max} in at.%.

ϕ	D[a]	C_{max}[a]	$F(\tau)$	$\bar{r}_b$[b]	$\langle \bar{r}_b \rangle$[b]	n_{Ne}[b,c]
			Mo backing[d]			
0.62	0.57	0.81 ± 0.04	35.6 ± 0.9	3.1	2.8	0.114
1.9	1.3	1.73 ± 0.09	34.5 ± 0.9	4.1	3.8	0.109
5.6	4.2	6.9 ± 0.3	34.7 ± 0.5	6.4	5.7	0.101
9.4	7.9	10.8 ± 0.5	35.4 ± 0.5	8.1	7.4	0.093
31	16	27.0 ± 1.1	39.4 ± 0.7	13	12[e]	0.077
94	18	25.8 ± 1.0	38.9 ± 0.7	13	12[e]	0.076
			Ta backing			
0.63	0.31	0.63 ± 0.05	32.2 ± 2.0	4.3	3.8	0.109
4.0	1.8	3.87 ± 0.09	32.0 ± 1.2	7.7	6.9	0.095
15	7.0	13.7 ± 0.7	33.1 ± 1.2	13	11	0.078
30	12	25.1 ± 0.7	35.1 ± 1.1	16	14	0.071
50	15	28.2 ± 1.1	38.1 ± 1.1	24	19[e]	0.065
94	14	27.0 ± 1.1	38.2 ± 1.2	24	18[e]	0.066
			Ta_2O_5 backing			
0.63	0.3	0.39 ± 0.04	38.7 ± 1.0		25[e]	0.060
4.0	2.2	3.03 ± 0.08	41.1 ± 1.2		30[e]	0.057
15	7.6	11.9 ± 0.9	52.0 ± 1.1		100[e]	0.030
30	9.1	12.5 ± 1.0	61.0 ± 1.3		230[e]	0.018
50	9.3	11.2 ± 1.0	63.0 ± 1.4		260[e]	0.016
94	11	10.8 ± 1.0	60.9 ± 1.3		230[e]	0.018

[a]Obtained in the measurements with the Rutherford backscattering (RBS) and nuclear-resonance-broadening (NRB) methods (for details see Ref. 4). The concentration is the average over about 25 nm due to the depth resolution of NRB at the depth of the maximum.
[b]The uncertainty of 20% includes the statistical error of the $F(\tau)$ values, the uncertainty in the $\bar{r}_b$-n_{Ne} relationship (Mo and Ta) in the assumption of Ne bubbles of only one size (Ta_2O_5) and in the stopping power. The systematic error (less than 20%) due to the portion of Ne not contained in bubbles is not included (see text).
[c]Values are given for $\langle \bar{r}_b \rangle$.
[d]The experimental data are from Ref. 4.
[e]Bubble coalescence (see text).

results of the calculations by Trinkaus and co-workers,[10] where the high-density equation of state of He was applied to He bubbles in Al and Ni and by the recent data[3] for Ne bubbles in Al. The 25% uncertainty in the theoretical $\bar{r}_b$-n_{Ne} relationship[10] was observed to produce 10% uncertainty in the $\bar{r}_b$ and 30% uncertainty in the C_b values.

The experimental data[12] on He in the amorphous alloy Fe-Ni-Mo-B show that the bubble density does not saturate to a constant value as in polycrystalline materials. Furthermore, the $F(\tau)$ values indicate that in Ta_2O_5 the bubble coalescence takes place already at low concentrations. Thus the concentration-dependent bubble density was obtained according to the formula

$$C_b(C) = \frac{n_0 C}{\bar{V}_b[(100-C)n_{Ne} + Cn_0]} , \quad (2)$$

where $\bar{V}_b = 4\pi\langle \bar{r}_b \rangle^3/3$, the bubble radius $\langle \bar{r}_b \rangle$ is the average over all concentrations probed by the recoiling ^{23}Na (a free parameter in the calculations), C (in at.%) is the Ne concentration, n_0 (Å^{-3}) is the atomic density of Ta_2O_5, and n_{Ne} (Å^{-3}) is the Ne density in bubbles. The fact that the recoiling ^{23}Na atoms emit γ rays around the maximum concentration, together with the results obtained at different concentrations, reduce uncertainty in $\langle \bar{r}_b \rangle$ to 15%.

The calculation of the $F(\tau)$ value has been described previously.[4] The slowing down of the recoiling ^{23}Na atoms was calculated with the correction parameters $f_n = 0.78 \pm 0.07$ for the nuclear stopping and $f_e = 1.00 \pm 0.17$ for the electronic stopping in Mo (Ref. 4), $f_n = 0.70 \pm 0.07$, $f_e = 1.15 \pm 0.15$ in Ta (reanalyzed values from Ref. 13), and $f_n = f_e = 1$ in Ta_2O_5 and ^{22}Ne. The uncertainties in the C_b and $\bar{r}_b$ values due to the uncertainties in the stopping powers are 30% and 10%, respectively. The recoiling ^{23}Na atoms are produced inside a Ne bubble at a distance of $P^{1/3}\bar{r}_b$ from the center, where the random number P is $0 < P < 1$. At this point the polar angles θ and ϕ of the center are given by

$$\theta = \arccos(1-2P_1) , \quad \phi = 2\pi P_2 , \quad (3)$$

where P_1 and P_2 are random numbers. The distance traveled by ^{23}Na before penetrating to a succeeding bubble is given by

$$d = -(C_b \pi \bar{r}_b^2)^{-1} \ln P - (\bar{r}_b^2 - \bar{y}_b^2)^{1/2} , \quad (4)$$

where $\bar{y}_b = P^{1/2}\bar{r}_b$ is the impact parameter determined at the original point.

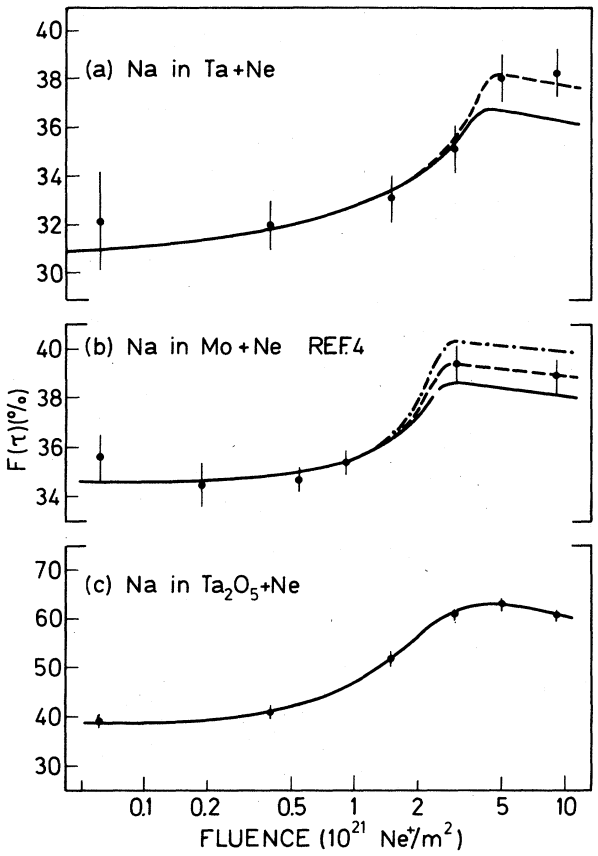

FIG. 1. Experimental $F(\tau)$ values for various fluences of 60-keV Ne^+ in (a) Ta, (b) Mo, and (c) Ta_2O_5. The solid lines show the $F(\tau)$ values calculated as a function of the bubble radius. The dashed lines in (a) and (b) are obtained by assuming the bubble coalescence which reproduces the experimental $F(\tau)$ values (see text). The point dashed line in (b) is obtained by assuming the coalescence of two Ne bubbles.

Bubble sizes obtained with the bubble densities $C_b = (3.6 \pm 1.8) \times 10^{25}$ m^{-3} and $(1.2 \pm 0.6) \times 10^{25}$ m^{-3} in Mo and Ta, respectively, are given in Table I. The systematic error due to the Ne not contained in bubbles is not included in the error limits. The fifth column shows $\bar{r}_b$ at the maximum concentration and the sixth column shows the mean radius $\langle \bar{r}_b \rangle$ probed by the recoiling ^{23}Na atoms around the maximum concentration. It is evident that bubbles in Mo are smaller than in Ta and that the growth is slower. The calculated $F(\tau)$ values are illustrated by the solid lines in Fig. 1. It can be seen that at the saturation concentrations [fluence $\phi > 3 \times 10^{21}$ (Ne^+ ions)/m^2 in Mo and $\phi > 5 \times 10^{21}$ (Ne^+ ions)/m^2 in Ta], the experimental $F(\tau)$ values are higher than the calculated ones. This indicates a decrease in the atomic density due to the bubble coalescence. The experimental $F(\tau)$ values were reproduced by the fitted bubble densities $C_b = (2.5 \pm 1.3) \times 10^{25}$ m^{-3} (Mo) and $(0.6 \pm 0.3) \times 10^{25}$ m^{-3} (Ta) and the increased bubble radii (Table I). In deriving these radii the bubble surface area was assumed to be conserved[14] $\bar{r}_b$ (coalescence) $= \sqrt{2}\,\bar{r}_b$. The results indicate that on the average two Ne bubbles coalesce in Ta, whereas in Mo this would yield considerably higher $F(\tau)$ values than observed (Fig. 1). Note, however, that the assumption holding for an ideal gas probably does not give consistent C_b and $\bar{r}_b$ values.

The present values $C_b = (2.5 \pm 1.3) \times 10^{25}$ m^{-3} and $\langle \bar{r}_b \rangle = 12 \pm 3$ Å obtained for Mo at $\phi = 31 \times 10^{20}$ (Ne^+ ions)/m^2 [dose 16×10^{20} (Ne atoms)/m^2] are not in disagreement with the values[15] $C_b \approx 1.5 \times 10^{25}$ m^{-3} and $r_b \approx 12$ Å for $\phi = 30 \times 10^{20}$ (He^+ions)/m^2 in Mo. No He data are available for Ta.

If for Ne an empirical formula of the form as proposed for the pressure-density relation[16] of He is used, the present atomic densities indicate overpressurized bubbles in Mo (e.g., 88 kbar for $\langle \bar{r}_b \rangle = 5.7$ Å) and Ta (e.g., 64 kbar for $\langle \bar{r}_b \rangle = 6.9$ Å). As already indicated by the partial coalescence, bubbles in Mo have relative high pressure also above the critical dose (e.g., 25 kbar for $\langle \bar{r}_b \rangle = 12$ Å). In comparison with the recent values[3] for Ne bubbles in Al (Ne concentration about 3 at.%), which are in agreement with the He data[10] in Al, the present values show that in metals with essentially higher elasticity moduli[17] (2.8×10^{10} kg m^{-2} for Mo, 1.9×10^{10} kg m^{-2} for Ta, to be compared with 0.7×10^{10} kg m^{-2} for Al) bubble sizes are considerably smaller and atomic densities and Ne pressures higher. The present and previous[3] data indicate that Ne bubble sizes at a constant concentration are inversely proportional to the elasticity moduli. In Ta_2O_5 the pressure values 11 kbar ($\langle \bar{r}_b \rangle = 25$ Å) to 1.1 kbar ($\langle \bar{r}_b \rangle = 260$ Å) show that there are no overpressurized bubbles, as can be expected on the basis of He data in an amorphous material[12] and the rapid growth of bubbles indicated by the fast increase of the $F(\tau)$ values. However, the Ta_2O_5 data demonstrate the high atomic density and pressure values obtained in Mo and Ta under the same experimental circumstances.

In conclusion, the first systematic data on non-He inert gas bubbles indicate a strong concentration dependence of the growth and pressure of Ne bubbles in heavy metals Mo and Ta and in comparison with the Ta_2O_5 data a high pressure in the bubbles.

[1] B. M. U. Scherzer, in *Sputtering by Particle Bombardment II*, edited by R. Behrisch, Topics in Applied Physics, Vol. 52 (Springer, New York, 1983), pp. 271-355.

[2] J. vom den Driesch and P. Jung, High Temp. High Pressures **12**, 635 (1980).

[3] A. vom Felde, J. Fink, Th. Müller-Heinzerling, J. Pflüger, B. Scheerer, G. Linker, and D. Kaletta, Phys. Rev. Lett. **53**, 922 (1984).

[4] J. Keinonen, A. Luukkainen, A. Anttila, and M. Erola, Nucl. Instrum. Methods **216**, 249 (1983).

[5] H. H. Andersen and H. L. Bay, in *Sputtering by Particle Bombardment I*, edited by R. Behrisch, Topics in Applied Physics, Vol. 47 (Springer, New York, 1981), pp. 145–218.

[6] J. Keinonen, in *Capture Gamma-Ray Spectroscopy and Related Topics—1984 (Knoxville)*, AIP Conf. Proc. No. 125, edited by S. Raman (AIP, New York, 1985), pp. 557–569.

[7]H. Van Swijgenhoven, G. Knuyt, J. Vanoppen, and L. M. Stals, J. Nucl. Mater. **114**, 157 (1983).
[8]R. Manzke, G. Crecelius, J. Fink, H. Trinkaus, and W. Jäger, J. Phys. F **12**, L279 (1982).
[9]P. B. Johnson and D. J. Mazey, J. Nucl. Mater. **111-112**, 681 (1982).
[10]H. Trinkaus, Radiat. Eff. **78**, 189 (1983); W. Jäger, R. Manzke, H. Trinkaus, G. Grecolius, R. Zeller, J. Fink, and H. L. Bay, J. Nucl. Mater. **111-112**, 674 (1982).
[11]C. J. Smitchells, *Metal Reference Book I, II, III* (Butterworths, London, 1976).
[12]H. Van Swijgenhoven, L. M. Stals, and G. Knuyt, J. Nucl. Mater. **118**, 125 (1983).
[13]A. Anttila, M. Bister, and J. Keinonen, Z. Phys. A **274**, 227 (1975).
[14]R. S. Barnes, D. J. Maxey: Proc. R. Soc. London, Ser. A **275**, 47 (1963).
[15]D. J. Mazey, B. L. Eyre, J. H. Evens, S. K. Erents, and G. M. McCracken, J. Nucl. Mater. **64**, 145 (1977).
[16]J. S. Rawlinson, Mat. Phys. **7**, 349 (1963/1964).
[17]*Handbook of Material Science,* edited by C. T. Lynch (CRC Press, Cleveland, 1974), Vol. 1, pp. 63–65.